image processing, immunogold labeling,
electron microscopy

Bartłomiej PŁACZEK[1], Rafał J. BUŁDAK[2,3], Renata POLANIAK[3],
Natalia MATYSIAK[4], Łukasz MIELAŃCZYK[4], Romuald WOJNICZ[4]

DETECTION OF IMMUNOGOLD MARKERS IN IMAGES OBTAINED FROM TRANSMISSION ELECTRON MICROSCOPY

In this paper a method is introduced which enables automatic detection of immunogold markers in transmission electron micrographs. Immunogold markers are used in electron microscopy to determine sub-cellular location of biological relevant macromolecules, such as proteins, lipids, carbohydrates, and nucleic acids. The proposed method combines image segmentation and feature localization approaches to improve accuracy of the immunogold markers detection in low contrast and highly textured image regions. A segmentation algorithm is intended in this study, which applies a flood-fill morphological operation. Accuracy of this method was evaluated by using electron microscopy images of human colorectal carcinoma cells. The experimental results show that the introduced method enables detection of immunogold markers with low false positive and false negative rates.

1. INTRODUCTION

Immunogold labeling technique is used in electron microscopy for staining of specific protein or cell component [9], [6], [10]. In this technique, immunoglobulin is allowed to react with an antigen and subsequently colloidal gold particles are bound to the specific immunoglobulin, which bind the target component using a second immunoglobulin or Protein A. The gold particles are used for their high electron density, which increases electron scatter to give dark circular markers. Immunogold labeling enables in situ localization of cellular macromolecules at the cellular and sub-cellular level. The obtained information is used to elucidate biochemical properties and functions of cellular components.

Immunogold markers in micrographs show the location of biological relevant macromolecules, such as: proteins, lipids, carbohydrates, and nucleic acids. The number, distribution, and spatial density of gold markers associated with cell structures are useful measures that report important information about the target macromolecules [6], [10], [2]. Manual localization and counting of the immunogold markers is time-consuming, biased, and poorly reproducible [13],

[1] Institute of Computer Science, University of Silesia, Sosnowiec, Poland, email: placzek.bartlomiej@gmail.com
[2] Department of Physiology, School of Medicine with the Division of Dentistry, Medical University of Silesia, Zabrze, Poland
[3] Department of Human Nutrition, School of Public Health, Medical University of Silesia, Zabrze, Poland
[4] Department of Histology and Embryology, School of Medicine with the Division of Dentistry, Medical University of Silesia, Zabrze, Poland

[12]. Therefore, automatic methods are necessary that allow the immunogold markers to be effectively and accurately detected.

In the literature, only few image processing methods have been proposed that enable semi-automatic or automatic detection of the immunogold markers in electron microscopy images. An early method, which was introduced by Starink et al. [12], enables markers segmentation by using edge detection and region growing. However, that method requires manual tuning of the region growing parameters and correction of the detection results. Another semi-automated method [3] applies morphological operations and interactive threshold selection to segment the markers. Monteiro-Leal et al. [5] have used a binary thresholding with user-selected threshold values to obtain foreground regions, which are then categorized based on their shape and size as small markers, large markers, or clusters of markers. Gaussian kernel was used as a synthetic prototype of the immunogold marker in [1]. According to that method, a correlation image is computed using the marker prototype and then a hysteresis thresholding is applied on the correlation image for marker detection. Detected candidate markers with a low circularity coefficient are removed to reduce the false positive error rate. The recent approach reported in [13] utilizes a multi-scale difference-of-Gaussians image representation to detect and categorize the markers. A Hessian matrix analysis is performed in that method to remove false detections that occur at strong edges or ridges.

The aforementioned state-of-the art methods are based on either image segmentation [12], [3], [5] or feature localization [13], [1]. In this paper a method is introduced which combines the image segmentation and feature localization approaches to improve accuracy of the immunogold markers detection in low contrast and highly textured image regions. According to the proposed method two sets of candidate marker locations are determined. The first set includes locations of markers recognized by using the difference-of-Gaussians approach. The second set is obtained as a result of image segmentation. These sets are then merged together to reduce the detection error. A segmentation algorithm is intended in this study, which applies a flood-fill morphological operation. Accuracy of the proposed detection method was evaluated by using electron microscopy images of human colorectal carcinoma cells.

The paper is organized as follows. Details of the proposed immunogold marker detection method are presented in Section 2. Section 3 includes results of the experimental evaluation. Finally, conclusions and future research directions are discussed in Section 4.

2. PROPOSED METHOD

The proposed algorithm for segmentation of micrographs with immunogold markers is based on a flood-fill morphological operation [11], which removes holes (local minima) in images. A hole in a greyscale image is defined as an area of dark pixels surrounded by lighter pixels. This operation brings the intensity values of dark areas that are surrounded by lighter areas up to the same intensity level as surrounding pixels. In effect, the holes are removed that are not connected to the image border. Since the immunogold markers appear as small dark areas, they correspond to the holes in the input image I. The candidate markers have to be localised in areas, where high intensity values are obtained for a difference image D:

$$D(x, y) = fill(I(x, y)) - I(x, y), \tag{1}$$

where $fill$ denotes the flood-fill operation.

Additionally, in the proposed segmentation algorithm, the fact is exploited that the markers colour is close to black. Thus intensities in the input image for marker locations have to be low. The two above conditions (low intensity in input image and high intensity in difference image) are taken into account by using thresholds α and β during segmentation. A binary image B,

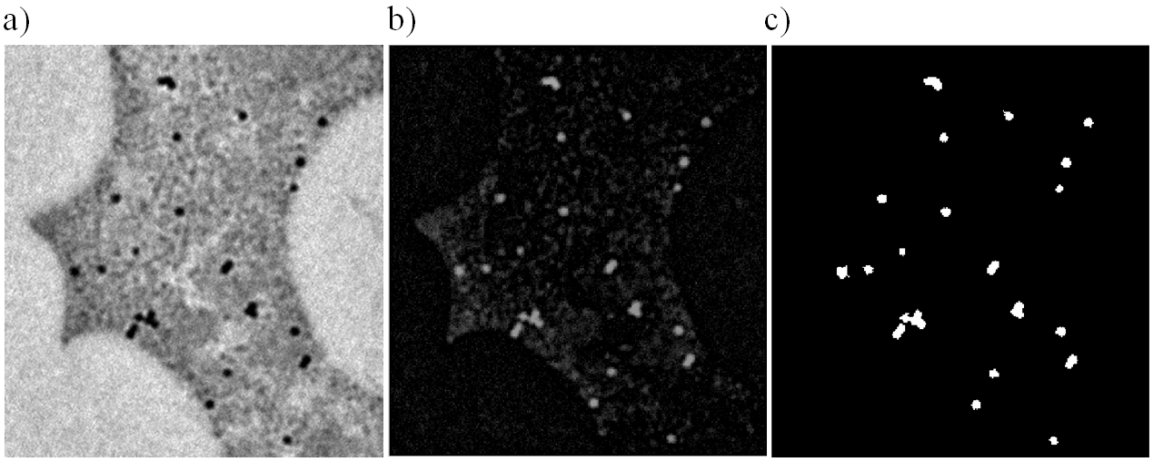

Fig. 1. Image segmentation: a) input image I, b) difference image D, c) binary image B.

which indicates the candidate marker locations, is determined as follows:

$$B(x,y) = \begin{cases} 1, & I(x,y) < \alpha \wedge D(x,y) > \beta, \\ 0, & \text{else.} \end{cases} \tag{2}$$

An example of the image segmentation is presented in Fig.1. Connected components in the binary image B are labelled and then the foreground (white) image regions with areas below a predetermined minimum or above a given maximum are removed.

In parallel, the candidate marker locations are recognized by using the multi-scale image representation, which is based on the difference-of-Gaussians (DoG) filtering [4]. The candidate marker positions correspond to local maxima at a scale level σ of the image representation R:

$$R(\sigma,x,y) = G(\sigma,x,y) * (1 - I(x,y)) - G(\sqrt{2}\sigma,x,y) * (1 - I(x,y)), \tag{3}$$

where $*$ denotes the convolution operation,

$$G(\sigma,x,y) = \frac{1}{2\pi\sigma^2} \exp\left\{-\frac{x^2+y^2}{2\sigma^2}\right\} \tag{4}$$

is the Gaussian kernel and σ can be determined on the basis of a known radius r of the circular markers [13]:

$$\sigma = 0.6\, r. \tag{5}$$

A local maximum is taken into consideration if the value of $R(\sigma,x,y)$ is above a given threshold τ. Finally, a local maximum in $R(\sigma,x,y)$ is categorized as a detected location of an immunogold marker if the pixel (x,y) is also recognized as a candidate marker location during the segmentation procedure. It means that the local maxima are ignored if they do not coincide with the segmented marker regions.

3. EXPERIMENTAL EVALUATION

Experiments were conducted in order to evaluate accuracy of the proposed method and compare it against the recent approach from the literature, in which false positive detections are eliminated on the basis of the local Hessian analysis [13]. For both compared methods, the DoG filtering is used to detect the candidate marker locations. In case of the proposed method, results of the DoG filtering are merged with the segmentation results, as discussed in Sect. 2. According to the method from literature, a local Hessian analysis is performed to

eliminate false detections at edges and ridges. A candidate marker at pixel (x, y) is discarded, if the following inequality is satisfied:

$$\frac{\mathrm{Tr}^2(\mathbf{H})}{\mathrm{Det}(\mathbf{H})} < \frac{(\rho+1)^2}{\rho} \tag{6}$$

where ρ is a parameter of the algorithm and $\mathbf{H}$ is the Hessian matrix calculated for pixel (x, y) of the image representation R at scale level σ:

$$\mathbf{H} = \begin{bmatrix} R_{xx} & R_{xy} \\ R_{xy} & R_{yy} \end{bmatrix}. \tag{7}$$

In case of $\rho = 1$, the condition (6) is satisfied only for ideal, radially symmetric markers. When a higher value of ρ is used then the inequality (6) holds also for more elongated structures.

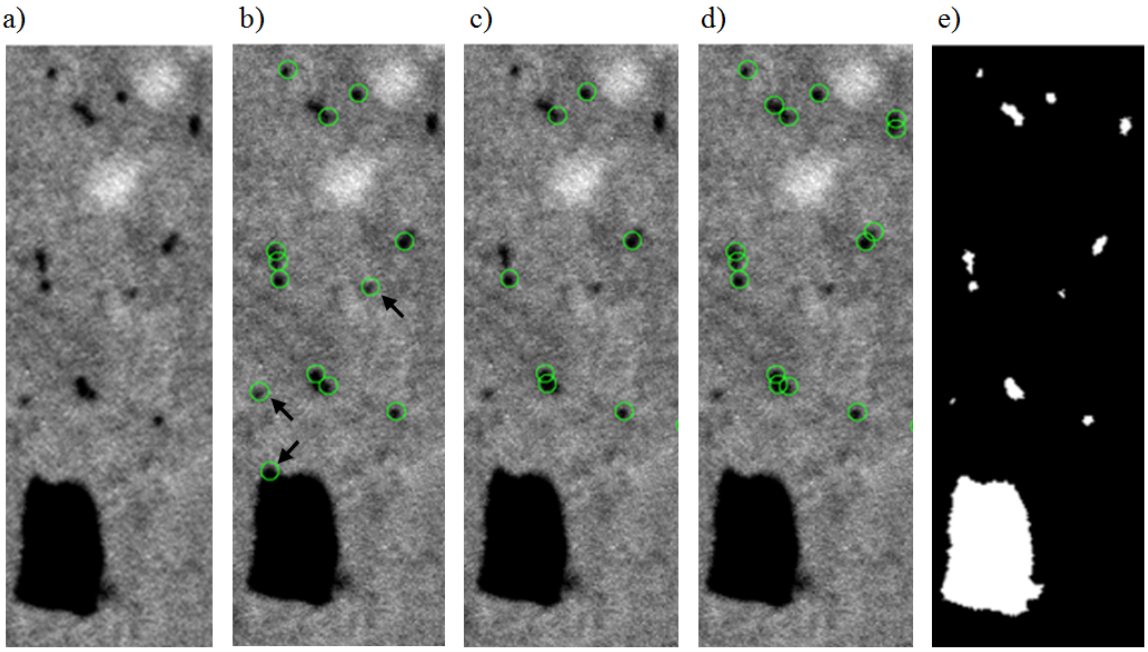

Fig. 2. Comparison of the detection results: a) test image with immunogold markers, b) markers detection with Hessian analysis ($\rho = 1.5$), c) markers detection with Hessian analysis ($\rho = 3$), d) markers detected for the proposed method, e) segmentation results (binary image B).

In this study, test images were used that show immunogold markers in human colorectal HCT-116 carcinoma cells. The cells were obtained from the American Type Culture Collection (ATCC). Immunogold labelling for TEM was performed to detect sub-cellular localization of visfatin [4]. The test images were acquired from FEI Tecnai G2 BioTWIN transmission electron microscope (FEI, Netherlands) at 120 kV and 16000x magnification using Morada CCD camera (Olympus, Hamburg, Germany). Radius of the immunogold markers in the test images corresponds to 3 pixels ($r = 3$).

Based on preliminary results, the threshold parameter τ of local maxima detection in $R(\sigma, x, y)$ was set to 0.4 for all experiments. Figure 2 shows examples of the results obtained by using the compared detection methods. For the method based on Hessian analysis, applied with $\rho = 1.5$, there are three false positive detections, as indicated by the arrows (Fig. 2 b). Moreover, in this example several immunogold markers remain undetected (top part of Fig. 2 b). The false positive detections can be eliminated by increasing the value of ρ, however for higher ρ values the number of false negative detections expands (Fig. 2 c).

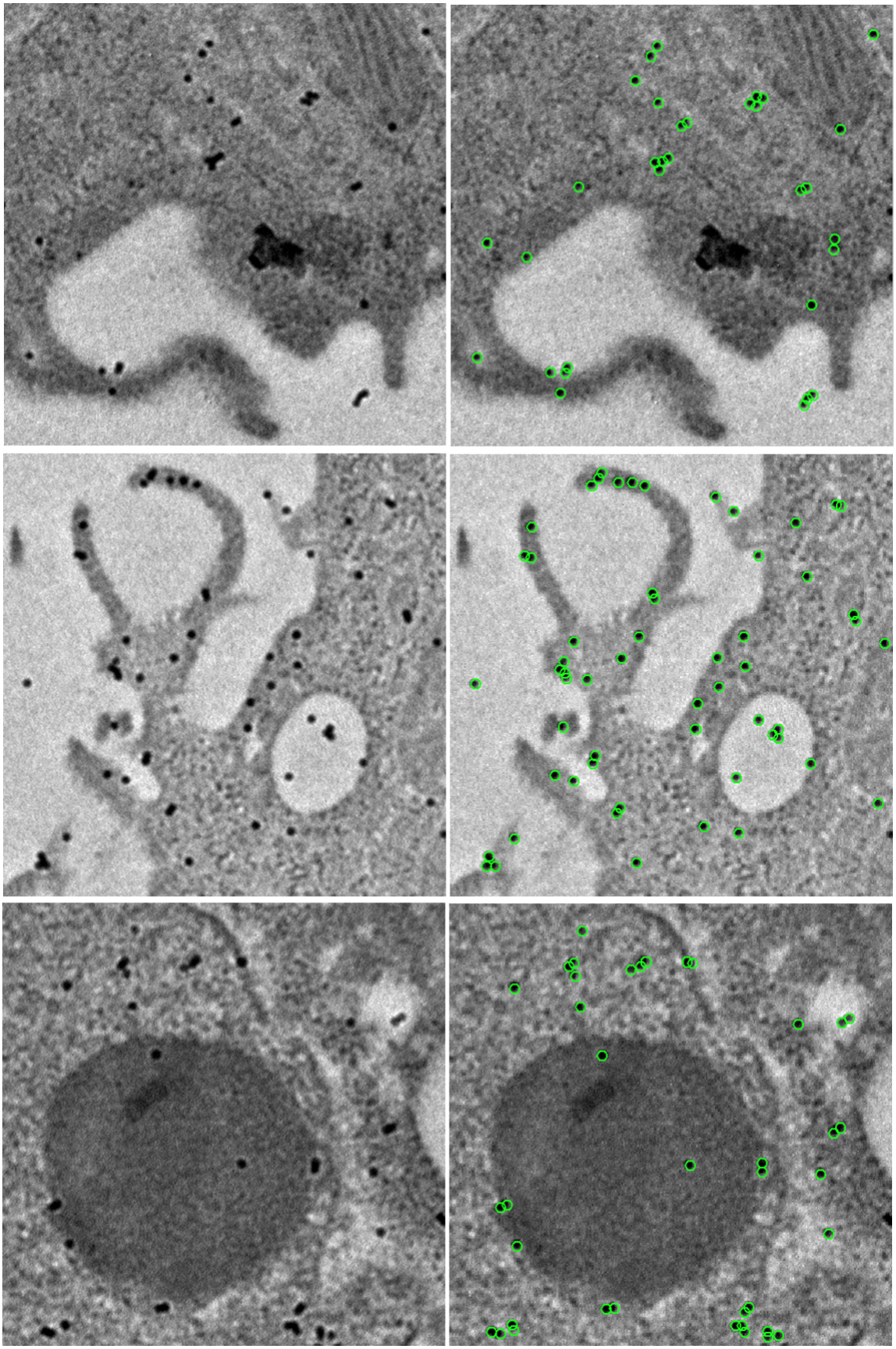

Fig. 3. Examples of the immunogold markers detection results for the proposed method.

According to the proposed method, the segmentation is performed instead of the Hessian analysis to improve the effectiveness of the immunogold marker detection. Results of the test image segmentation are presented in Fig. 2 e. In the segmented image, the foreground regions with areas below 5 pixels or above 200 pixels are removed. The values of maximum and minimum area parameters were determined during preliminary experiments. For the analysed example, the proposed method enables correct detection of all markers (Fig. 2 d).

Accuracy of the examined methods was evaluated using a set of test images that include over 1500 immunogold markers. Examples of these images as well as detection results for the proposed method are shown in Fig. 3. By using the introduced method, the markers were successfully detected in low contrast and highly textured image regions. The summary test results are presented in Tab. 1. Both the false positive rate and the false negative rate are lower for the proposed method than for the state-of-the-art method, which is based on Hessian analysis.

Table 1. Accuracy of immunogold marker detection.

	False positives per 100 markers	False negatives per 100 markers
Proposed method	3.6	2.9
Hessian-based method	5.1	4.8

4. CONCLUSIONS

The proposed method combines image segmentation and feature localization approaches to improve the accuracy of immunogold markers detection in low contrast and highly textured micrographs. A segmentation method is proposed based on morphological operations. Experimental testing was performed on a set of images obtained from transmission electron microscopy. The test micrographs show immunogold markers in human colorectal carcinoma cells. Results of the experiments reveal higher accuracy of the proposed method in comparison to a state-of-the-art approach. Further research challenges include automatic recognition of markers size as well as improvements of the segmentation method based on applications of cellular automata [7] and fuzzy descriptors of image regions [8].

BIBLIOGRAPHY

[1] BRANDT S., HEIKKONEN J., ENGELHARDT P., Multiphase method for automatic alignment of transmission electron microscope images using markers. Journal of structural biology, 2001, Vol. 133 (1), pp. 10-22.

[2] BUŁDAK R. J., SKONIECZNA M., MATYSIAK N., WYROBIEC G., KUKLA M., MICHALSKI M., SWIRSKA-KORCZALA K., Changes in subcellular localization of visfatin in human colorectal HCT-116 carcinoma cell line after cytochalasin B treatment. European Journal of Histochemistry, 2014, Vol. 58 (3), pp. 239-246.

[3] LEBONVALLET S., MENNESSON T., BONNET N., GIROD S., PLOTKOWSKI C., HINNRASKY J., PUCHELLE E., Semi-automatic quantitation of dense markers in cytochemistry. Histochemistry, 1991, Vol. 96 (3), pp. 245-250.

[4] LOWE D. G., Distinctive image features from scale-invariant keypoints. International journal of computer vision, 2004, Vol. 60 (2), pp. 91-110.

[5] MONTEIRO-LEAL L. H., TROSTER H., CAMPANATI L., SPRING H., TRENDELENBURG M. F., Gold finder: a computer method for fast automatic double gold labeling detection, counting, and color overlay in electron microscopic images. Journal of Structural Biology 141, 2003, pp. 228–239.

[6] NEJATBAKHSH R., KABIR-SALMANI M., DIMITRIADIS E., et al., Subcellular localization of L-selectin ligand in the endometrium implies a novel function for pinopodes in endometrial receptivity. Reprod Biol Endocrinol, 10:46, 2012, pp. 1-9.

[7] PŁACZEK B., Rough sets in identification of cellular automata for medical image processing. J. Med. Inf. Technol, 2013, Vol. 22, pp. 161-168.

[8] PŁACZEK B., Vehicles recognition using fuzzy descriptors of image segments. In Computer Recognition Systems 3, Springer Berlin Heidelberg, 2009, pp. 79-86.

[9] SALUJA R., JYOTI A., CHATTERJEE M., HABIB S., et al., Molecular and biochemical characterization of nitric oxide synthase isoforms and their intracellular distribution in human peripheral blood mononuclear cells. Biochimica et Biophysica Acta (BBA)-Molecular Cell Research, 2011, Vol. 1813 (10), pp. 1700-1707.
[10] SHIMIZU Y., KABIR-SALMANI M., AZADBAKHT M., SUGIHARA K., SAKAI K., IWASHITA M., Expression and localization of galectin-9 in the human uterodome. Endocrine journal, 2008, Vol. 55 (5), pp. 879-887.
[11] SOILLE P., Morphological Image Analysis: Principles and Applications, Springer-Verlag, 1999, pp. 173-174.
[12] STARINK J. P., HUMBEL B. M., VERKLEIJ A. J., Three-dimensional localization of immunogold markers using two tilted electron microscope recordings. Biophysical journal, 1995, Vol. 68 (5), pp. 2171-2180.
[13] WANG R., POKHARIYA H., MCKENNA S. J., LUCOCQ J., Changes in subcellular localization of visfatin in human colorectal HCT-116 carcinoma cell line after cytochalasin B treatment. Recognition of immunogold markers in electron micrographs. Journal of structural biology, 2011, Vol. 176 (2), pp. 151-158.